Westfälische Wilhelms-Universität Münster

GEOPHYSIK WWU MÜNSTER

Processing and analysis of CSEM data acquired at a test site near Herford using Impressed Pipeline Currents as a source

T. Lindau, M. Becken, Institute of Geophysics, WWU Münster

Introduction

Impressed Current Cathodic Protection (ICCP) systems are extensively used for the protection of central Europe's dense network of oil-, gas- and water pipelines against destruction by electrochemical corrosion. Protection is provided by the injection of a DC current into the pipeline (Figure 2). However, occasional pipeline integrity surveys demand the protection current to be switched on- and off periodically. The resulting time varying pipe current induces secondary electric- and magnetic fields in the surrounding earth. While these fields are usually considered to be unwanted cultural noise, we aim at utilizing these fields for EM exploration, since the switching cycles typical fundamental periods roughly correspond to periods used in controlled source EM applications (CSEM).

We performed measurements on a test segment of 35km length near Herford, Germany (Figure 1) which is part of a gas pipeline operated by Westnetz. The DC current injected into the pipeline originates in a rectified 50Hz AC signal which can be switched on- and off periodically.

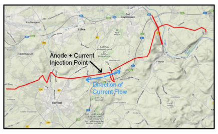

Figure 1: Map view of the test area with the pipeline path depicted in red. The current is injected in the approximate center of the pipe from where it is flowing towards both ends.
Source: maps.google.de

The switching pattern typically employed by the pipeline operators has a fundamental period of 15s (12s on and 3s off), but for our study we chose a pattern with a fundamental period of 30s (25s on and 5s off, Figure 4). In order to describe the pipeline in terms of an EM source it is necessary to determine the current distribution within the pipeline, since the current decays away from the injecton point (current leakage). In addition the injected current signal needs to be recorded.

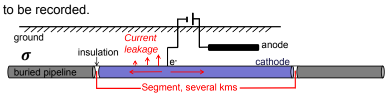

***Figure 2:** Depiction of a typical ICCP Setup. The pipeline is split into multiple, electrically isolated segments. Each segment is equipped with ist own ICCP system which consists of an anode and a DC power source. In addition the pipeline is protected by an isolating coating (e.g. bitumen). The coating may be damaged at various locations, causing the current to leak into the surrounding earth.*

Data

Electric field measurements were performed at 45+ stations in an area close to the pipeline and at the current injection point. Each station recorded data for approximately two days at 500Hz sampling rate using the inhouse developed EDE32 dataloggers

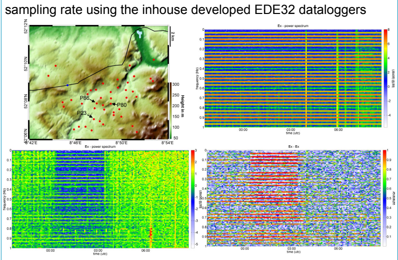

***Figure 3:** **Top Left:** Map view of measurement area. Red dots show measurement sites, the blue dot indicates the injection site. **Top Right:** Spectrum of the recorded pipeline signal at the injection point for frequencies up to 1Hz.The spectrum shows high powers for the pipelines fundamental period of 30s and its harmonics and low power elsewhere. **Bottom Left:** Ex power spectrum for station labeled P23 **Bottom Right:** Plot of coherency of injected current signal (Ex) and Ex component of measurement site P23.*

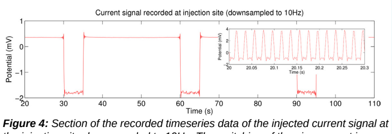

***Figure 4:** Section of the recorded timeseries data of the injected current signal at the injection site downsampled to 10Hz. The switching of the pipe current is clearly visible. The snippet shows the signal at the 512Hz sampling rate.*

Transfer Function Estimates

From the data we estimate transfer functions describing the relationship between the recorded electric field and the injected protection current as

$$\underbrace{\begin{pmatrix} E_x \\ E_y \end{pmatrix}}_{\vec{E}} = \underbrace{\begin{pmatrix} T_x \\ T_y \end{pmatrix}}_{\vec{T}} I \quad , \vec{T} = \vec{T_{\Re}} + \vec{T_{\Im}} = \text{Telluric Vector}$$

Where E is the recorded electric field vector, I the injected protection current and T the univariate transfer function. The transfer functions are estimated in the frequency domain using a regression M-estimate (e.g. Egbert and Booker, 1986) and the data used for the estimate is chosen based on coherency between the electric fields and the protection current. In addition only coefficients of frequencies associated with the pipeline signal are used. For synthetic data transfer functions are calculated by division of the electric fields by a factor corresponding to the known total injected current of 2.5A.

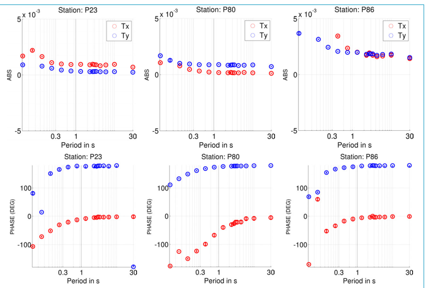

***Figure 5:** Example of transfer functions estimated from the data for the stations labeled P23, P80 and P86. The transfer functions are smooth. While P23 shows only little dependence of the phase on the frequency, P86 shows a strong dependence.*

Modeling and Inversion

The pipe current was measured at discrete points using a pipeline detection tool and was found to decay exponentially towards the ends. An exponential function fitted to the measured values is used to be able to determine the source current at arbitrary points along the pipeline. 1D modeling is performed using the software EM1D (Streich and Becken 2011a). The pipeline model consists of 510 finite wire sources to approximate the pipeline geometry (Streich and Becken 2011b) and the individual sources current is determined from the fit to the measured data. Figure 6 shows the transfer functions (real part) computed for our model and various subsurface models in conjunction with the transfer functions estimated from the data.

The lenght of the real telluric vector was inverted for single stations and homogeneous half spaces at two neighbouring frequencies. We assumed 5% data error and error floors of 1e-5. Examples of the resulting resistivities are plotted on a map (see Figure 8). The results are consistent for single stations over the whole frequency range (0.03 Hz – 3 Hz), but may lack spacial consistency. The length of the imaginary telluric vector could not be fitted.

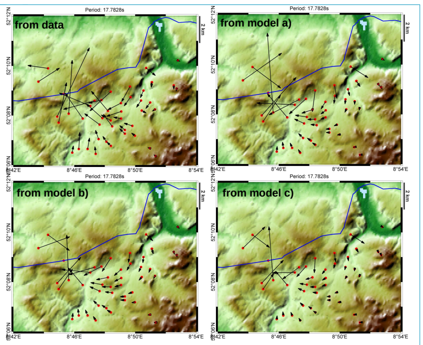

***Figure 6:** Arrows indicating the direction and length of the real telluric vector. **Top Left**: Transfer functions estimated from the data **Top Right**: Transfer functions calculated for model a) in Figure 7 **Bottom Left:** Transfer functions calculated for model b) in Figure 7 **Bottom Right:** Transfer functions calculated for model c) in Figure 7.*

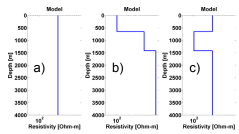

***Figure 7:** Models used to calculate the transfer functions shown in Figure 6. Model labeled a) corresponds to values shown in Figure 6 top right, b) to Figure 6 bottom left, and c) Figure 6 bottom right.*

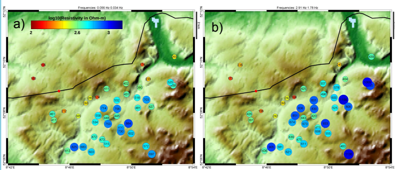

***Figure 8:** Results from inverting the length of the real telluric vector. Inversion was performed for each station separately and frequencies of **a)** 0.03 Hz and 0.06 Hz **b)** 1Hz and 3 Hz. The numbers give the half space resistivity in Ohm-m (also indicated by size and color of the circles).*

Inversion of the data for layered subsurface models for single stations or carefully chosen combinations of multiple stations were partially successful. Again, only the length of the real telluric vector could be fitted with 10% error assumption. The modelled data shows a frequency dependent amplitude comparable to the frequency dependence observed in the transfer functions estimated from the data (Figure 9).

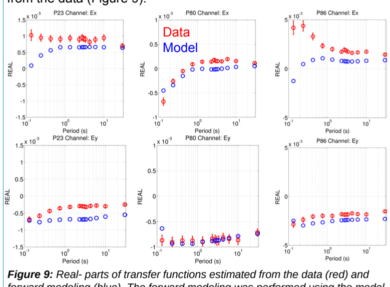

***Figure 9:** Real- parts of transfer functions estimated from the data (red) and forward modeling (blue). The forward modeling was performed using the model resulting from a single station 1D inversion of the measured data for the lenght of the real telluric vector. 10% errorbars are plotted for the measured data.*

Conclusion

- Signals originating from the ICCP current are clearly visible in the recorded electric field data
- Transfer functions obtained from modeling show similar behavior as the transfer functions estimated from the data
- Inversion of single station data for narrow frequency bands give reasonable apparent resistivities for the subsurface
- However, generally inverting the data for 1D resistivity models proves difficult
- The lenghts of the real telluric vector observed in the data can be matched by the synthetic models
- Further attempts aim at using improving the 1D inversions. Additionally, 3D inversion approaches will be used in order to fit both, the real- and imaginary- parts of the transfer function data, ideally for the whole dataset rather than single stations.

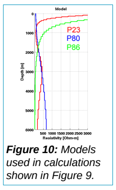

***Figure 10:** Models used in calculations shown in Figure 9.*

Literature

Egbert, G. D. and J. R. Booker (1986): Robust estimation of geomagnetic transfer functions. *Geophysical Journal of the Royal Astronomical Society* 87, 173-194

Streich, R. and M. Becken (2011a): Electromagnetic fields generated by finite-length wire sources: Comparison with point dipole solutions. *Geophysical Prospecting* 59(2), 361-374

Streich, R. and M. Becken (2011b): Sensitivity of controlled-source electromagnetic fields in planarly layered media. *Geophysical Journal International* 187(2), 705-728

living.knowledge
WWU Münster

Acknowledgements

We would like to thank Westnetz for technical support and access to their pipeline infrastructure.

We thank the Department of Geophysics at the University of Frankfurt for their hospitality and support.

This project is funded by the Germany Science Foundation (DFG) under grant BE 5149/2-1